Two-Phase Pressure Drop in Vertical Crossflow Across a Horizontal Tube Bundle

An experimental investigation has been made to evaluate the friction, acceleration, and hydrostatic pressure drops in two-phase vertical crossflow across a horizontal tube bundle through the measurement of the void fraction and determination of the two-phase friction multiplier. The void fractions were found to increase with increasing mass velocity for a fixed quality level. The two-phase friction multiplier increased with increasing mass velocity for a fixed value of the Martinelli parameter in both slug and spray flow and decreased with increasing mass velocity in bubbly flows. The void fraction and two-phase friction multiplier data were correlated and used to predict with very good results the total pressure drop occurring in simulated diabatic flow tests and in actual diabatic tests using R-113.

D. S. Schrage, J.-T. Hsu, M. K. Jensen
Department of Mechanical Engineering
University of Wisconsin
Milwaukee, WI 53201

Introduction

The two-phase pressure drop literature is extensive for in-tube and parallel flow geometries. However, only limited information is available for use in vertical, crossflow boiling. This is surprising given the wide industrial use of boiling on the shell side of tube bundles, such as in kettle reboilers. In kettle reboilers, a recirculating flow through the bundle is set up because of the density difference between the two-phase mixture in the bundle and the liquid outside the bundle. The flow is determined by a balance between the driving hydrostatic pressure head and the accelerational and frictional pressure drops. Because the heat transfer coefficients in kettle reboilers have been found to be functions of the flow past the tube, there is a complex coupling between the hydrodynamic and heat transfer processes. Thus, to model the thermal hydraulics in kettle reboilers, the three components of pressure drop—hydrostatic, friction, and acceleration—need to be known. To calculate the hydrostatic and acceleration pressure drops, the void fraction is needed. For the friction pressure drop, using a separated flow model, the two-phase friction multiplier is needed.

Previous research on pressure drop across tube bundles has been directed mainly toward horizontal flows (Chisholm, 1983; Diehl and Unruh, 1958; Grant and Chisholm, 1979). As a result, work on vertical two-phase crossflows has been hampered by lack of knowledge of the void fraction and two-phase friction multiplier. The only study that addressed the evaluation of the void fraction in vertical upflow (Kondo and Nakajima, 1980) was performed at such low mass velocities that the results are not generally usable. Some researchers (Fair and Klip, 1983; Palen and Yang, 1983; Payvar, 1983; Polley et al., 1981) have circumvented the problem of the lack of a suitable void fraction model by adopting in-tube void fraction models, but with no justification given for this procedure. Others (Leong and Cornwell, 1979; Whalley and Butterworth, 1983) have used the homogeneous model.

In comparison to the work that has been done on shell-side void fractions, there has been more attention given to the two-phase friction multiplier. Unfortunately, because of the lack of a valid void fraction model some researchers have used in-tube models (Grant et al., 1974; Fair and Klip, 1983; Polley et al., 1981) or the homogeneous model (Whalley and Butterworth, 1983); others failed to identify the void fraction model used (Diehl, 1957; Ishihara et al., 1979; Palen and Yang, 1983). Grant and Chisholm (1979) obtained adiabatic pressure drops from adjacent channels in a baffled heat exchanger and assumed that when the upflow pressure drop was added to the downflow pressure drop, the hydrostatic component of pressure drop was canceled using this procedure. Thus, a two-phase friction multiplier could be obtained without actually needing to use a void fraction. However, this procedure is valid only if the void fraction in the upflow section is identical to that in the downflow section; whether this is true or not is unknown.

Correspondence concerning this paper should be addressed to M. K. Jensen, Department of Mechanical Engineering, Aeronautical Engineering, and Mechanics, Rensselaer Polytechnic Institute, Troy, NY 12180.

Many investigators have used a Martinelli-type model to represent the two-phase friction multiplier:

$$\phi_\ell^2 = 1 + C/\chi_{tt} + 1/\chi_{tt}^2 \tag{1}$$

where

$$\chi_{tt}^2 = \left(\frac{1-x}{x}\right)^{2-m}\left(\frac{\rho_v}{\rho_\ell}\right)\left(\frac{\mu_\ell}{\mu_v}\right)^m \tag{2}$$

Different values have been given for the C factor in Eq. 1. After critically reviewing both two-phase friction multiplier data and models, Ishihara et al. (1979) fitted Eq. 1 to their data bank and obtained a value of 8 for the C factor when $m = 0.2$. This predicted the shear-controlled flow data for $\chi_{tt} < 0.2$ with good results; however, for $\chi_{tt} > 0.2$ deviations between the data and the predictions were quite large. Ishihara et al. concluded that to improve the correlation, flow pattern should be taken into account when evaluating the C factor.

This paper is concerned with the evaluation of the pressure drop in vertical two-phase crossflows over a horizontal tube bundle. The main objectives of the experimental study were to obtain void fractions and two-phase friction multipliers from adiabatic air-water mixtures for a range of flow conditions. One in-line tube bundle was tested. Quick-closing plate valves were used to isolate only the tube bundle to obtain a volume-average void fraction. This measurement then permitted the friction pressure drop to be backed out of the measured total pressure drop. The final objectives were to correlate the void fraction and two-phase friction multiplier data and to validate these correlations by comparison with actual diabatic total pressure drop data.

The measured void fractions were significantly lower than the homogeneous void fractions; at a fixed quality level, the void fraction increased with increasing mass velocity. The two-phase friction multiplier depended on both the mass velocity and flow pattern. Correlations developed for the void fraction and two-phase friction multiplier were then used to predict the total pressure drop from simulated diabatic flow tests (air injected at each tube row) and from actual diabatic flow tests using R-113. The agreement between the predictions and the experimental data was very good.

Experimental Apparatus and Procedure

Air-water mixtures were used to model two-phase adiabatic and simulated diabatic flows in the tube bundle. The difference between these two operating modes was the point of air injection: upstream of the tube bundle for the adiabatic tests and at each row for the simulated diabatic tests. A diagram of the flow loop is shown in Figure 1. Flow control valves were located in the air and water lines. A control valve was located in the exhaust piping and was used to control the backpressure on the test section. Since it was necessary to be able to instantaneously stop the flow of air and water and to divert the flows around the test section, electrically operated solenoid valves were also used in both the air and water lines. The air and water flow rates were measured with turbine flow meters at the higher flow rates and with rotameters at the lower flow rates. The pressure level in the tube bundle and in the air flowmeter were measured with Bourdon tube pressure gauges. Pressure drops in the test section were measured with five U-tube manometers which were modified so that each could be inclined from a vertical position for improved accuracy during low pressure drop measurements. The air temperature in the air flowmeter and the air-water mixture temperature were measured with copper-constantan thermocouples.

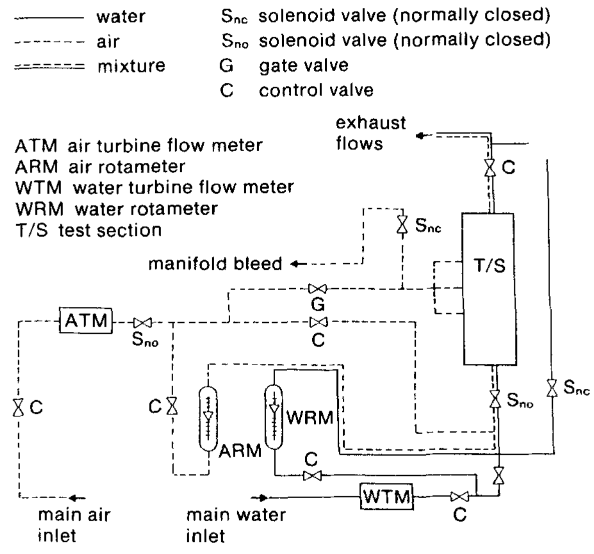

Figure 1. Flow loop.

The test section, diagrammed in Figure 2, consisted of a vertical rectangular channel. Solenoid-driven plate valves immediately upstream and downstream from the first and last rows of tubes in the bundle, respectively, were used to isolate the tube bundle from the inlet mixing section and the exit section. These plates slid through slots in the channel wall, were connected by a series of linkages, and were driven by a combination spring-solenoid unit. This combination provided enough force to quickly close the valves and to maintain enough force after closing to effectively seal the channel. The valve actions were synchronized through the use of a six-bar linkage. Microswitches were

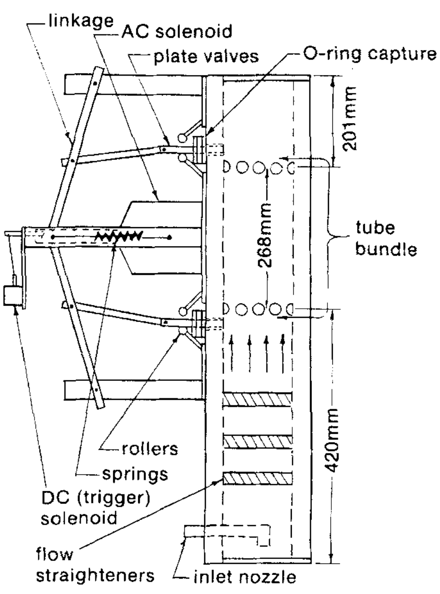

Figure 2. Test section.

attached to the solenoid plunger to measure the closing time of the plate valves. The mixing section consisted of an inlet nozzle at the entrance to the test section and a series of three flow straighteners and mixers. The section containing the tube bundle model was fitted with 27 rows of 7.94 mm dia. tubes with five tubes in each row. The in-line, square array had a pitch-to-diameter ratio of 1.3. To reduce bypass leakage and to minimize wall effects, the two walls parallel to the tube bank were machined such that the two outside columns of tubes had only one-half of the tube diameter exposed to the flow. Pressure taps were located in the side walls, so that five pressure drops (across six, five, five, five, and six rows) could be measured. The two columns of tubes located directly off the center column contained stainless steel tubes. Each of these tubes was drilled with two 1 mm holes, 2.54 cm from each end. The purpose of these holes, which were oriented directly downward, was to permit air injection into the flow all along the length of the bundle, thus simulating diabatic flow.

Single-phase pressure drop tests were taken with water to verify the experimental apparatus and procedure and to help reduce the two-phase results. The two-phase tests were run so that the total mass velocity was fixed as the quality was increased. In all the air-water tests, any air accumulation in the manometer lines was purged prior to recording the deflections so that accurate pressure drop recordings would be obtained. After recording all the flow data, the flow isolation plate valves were closed to make the void fraction measurement. The water that was trapped between the plate valves settled to some level, which was recorded. Any water clinging to the tubes above the water surface was taken into account when calculating the void fraction. To estimate the amount of water clinging to the tubes, a series of calibration tests was performed. These data were combined to estimate the void fraction in the tube bundle. Details of this are given by Schrage (1986). The pressure drop and void fraction measurement techniques were the same for both the adiabatic and simulated diabatic tests. To determine if the measured void fraction was affected by the plate valve closing time, measurements were made at various values of closing time. No significant variation in void fraction was measured for closing times from 0.035 to 0.50 s.

For the adiabatic flow tests, quality was constant across the test section. However, in the simulated diabatic flow tests there was a uniform addition of air to the water along the length of the tube bundle, which increased the total mass flow rate at each row. Because of the large pressure drop occurring between the inside and the outside of the tubes and because of the design of the air manifold, it was assumed that each row of tubes added $1/27$ of the total mass flow of air.

The single-phase friction factor was calculated with

$$f_{\ell t} = 2\Delta P_{F1\phi}\rho_\ell / MG_{\ell t}^2 \tag{3}$$

Because of the possibility of inlet and exit effects, the single-phase friction factors were computed between the second and third, third and fourth, and fourth and fifth pressure taps and then averaged. As in the calculation of the single-phase friction factor, the adiabatic two-phase friction multiplier was determined using pressure drop data between the second and fifth pressure taps. The two-phase friction multiplier based on the liquid phase flowing alone, ϕ_ℓ^2, was determined using this procedure also and was defined as:

$$\phi_\ell^2 = \frac{\Delta P_{F2\phi}}{\Delta P_{F\ell 1\phi}} = \frac{2\rho_\ell \Delta P_{F2\phi}}{Mf_\ell G_\ell^2} \tag{4}$$

The determination of the two-phase frictional pressure drop required that the acceleration and gravitational pressure drop components be subtracted from the total pressure drop. These two components were calculated using the measured void fraction.

In simulated diabatic flow tests the outlet mass velocity range was the same as that in the adiabatic tests. However, in this flow mode the addition of air to the flow stream resulted in a difference between the inlet and outlet mass velocities. At the highest outlet mass velocity this increase was less than 5%, while for combinations of high outlet quality and low outlet mass velocity, the mass velocity increased nearly 200% over the tube bundle.

The raw and reduced data for all tests and details of the apparatus and procedures can be found in Schrage (1986). The nominal range of experimental conditions covered in this investigation were:

$3.0 \times 10^{-4} \leq x \leq 0.68$
$55 \leq G \leq 680\ \mathrm{kg/m^2 \cdot s}$
$1 \leq P \leq 3$ atm

The mixture temperature was about 10°C for all tests. Uncertainties for the majority of the experimental data, as estimated through a propagation-of-error analysis, are suggested to be: G ±3%; x ±7%; α ±4%; ϕ_ℓ^2 ±4%. At low qualities and high mass velocities, the uncertainties in α and ϕ_ℓ^2 could be substantially greater than these values.

Results and Analysis

Single-phase friction factor

The single-phase friction factors for Reynolds numbers from 200 to 6,800 from this study were compared with the ESDU (1979) and Zhukauskas (1972) correlations and the data of both Frass and Ozisik (1965) and Kays and London (1984). Generally, there was close agreement between sources and the data for $Re > 1{,}000$; however, the deviation between the present data and the two correlations for $Re < 1{,}000$ was as high as 75% at the lowest Reynolds number. This was attributed to equipment limitations in measuring the very small pressure drops in this Reynolds number range. Except for the data for $Re < 1{,}000$, it was concluded that because there generally was close agreement between the data and the correlations, the tube bundle model used in this study was representative of the actual behavior encountered in larger bundles. The data from this study indicated the presence of a laminar and transition region; a turbulent region was not indicated by the data, but probably occurs at Reynolds numbers higher than those tested. To accurately represent the single-phase friction factor, a three part Blasius-type friction factor model was used to correlate the data.

Adiabatic void fraction

It was speculated that by comparing the measured adiabatic void fraction data with the homogeneous void fraction model, the type of flow model (separated or homogeneous) required to reduce the total pressure drop would be clearly indicated. In

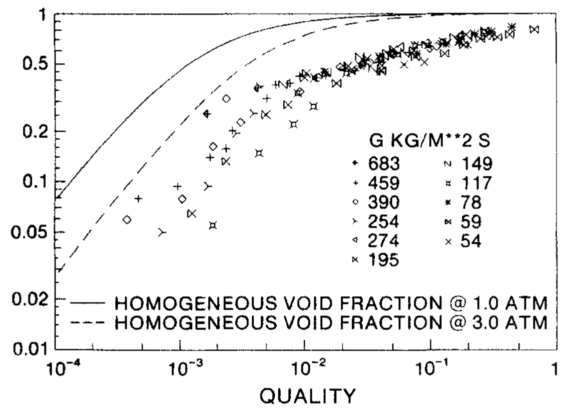

Figure 3. Void fraction data from present study.

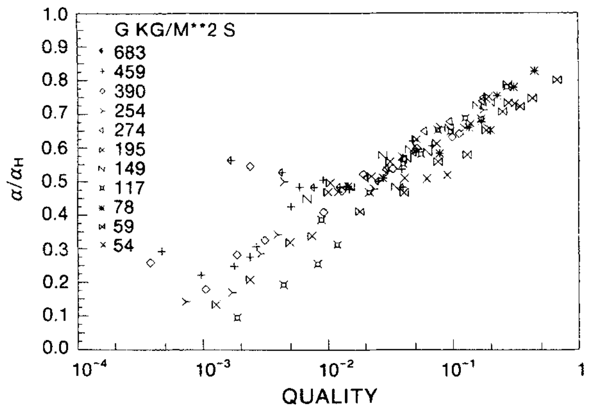

Figure 4. Effects of mass velocity on reduced void fraction.

Figure 3 the void fraction data and the homogeneous model at pressures of 1 and 3 atm have been plotted. As can be seen, the homogeneous void fraction model dramatically overpredicts the void fraction data for all quality and mass velocity levels. Although the general trends between the homogeneous model and the data are the same, the poor agreement indicates that the homogeneous flow model is not applicable. Thus, the separated flow model must be used.

In the present data, there was some scatter, which may be attributed in part to different pressure levels. To eliminate the effects of pressure, a reduced void fraction was used which was the ratio of the measured void fraction to the homogeneous void fraction evaluated at the same conditions. In Figure 4, the reduced void fraction clearly shows the mass velocity trends. As the mass velocity increased the reduced void fraction also increased; hence, the actual void fraction began to approach that of the homogeneous model. Note also that as quality approached unity the reduced void fraction tended to approach unity, which is an expected trend. However, as the quality approaches zero if the trend in the data is extrapolated, it appears that the reduced void fraction will approach zero at some finite quality, which is not possible. Based on the physics of the process, an argument can be made that as the quality tends toward zero, the reduced void fraction will approach unity after some minimum value is reached. If it is assumed that at very low qualities the gas phase is present in the form of very small bubbles, the flow will behave essentially as a homogeneous flow, the actual void fraction will approach the homogeneous void fraction, and hence the reduced void fraction will approach unity. The critical quality, after which for lower qualities the reduced void fraction would begin to increase, would tend to be higher for higher mass velocities since at higher mass velocities the flow would behave more homogeneously; for example, see the data for $G = 683$ kg/m$^2 \cdot$ s in Figure 4. This trend is suggested based on the observation of only a few data points and physical reasoning. Additional data are required to confirm these trends. Because of the lack of data it was impossible to fix the various combinations of quality and mass velocity at which the minima in the reduced void fraction curves occur. Thus, the minimum value of the reduced void fraction was assumed, somewhat arbitrarily for correlation purposes, to never be less than 0.1 for any combination of mass velocity and quality.

Utilizing the boundary condition at $x = 1.0$, $\alpha/\alpha_H = 1$, the reduced void fraction data were correlated as:

$$\alpha/\alpha_H = 1 + 0.360G^{-0.191} \ln x \tag{5}$$

This is a dimensional equation in G that requires the mass velocity to have units of kg/m$^2 \cdot$ s. Using the restriction on the reduced void fraction given above, the final void fraction model consisted of two parts. If the reduced void fraction predicted by Eq. 5 was less than 0.1, then $\alpha/\alpha_H = 0.1$; otherwise Eq. 5 would define the reduced void fraction.

A comparison of the final two-part void fraction model with the adiabatic data resulted in an average absolute deviation between the predictions and the experimental data of 10.3%, with 98 of the 108 data predicted with a deviation of less that ±20%. Note that for this curve fit, two data points were rejected by applying the criterion of Chauvenet (Holman, 1984). (This criterion is a technique by which outlying points can be rejected from the data set.) Figure 5 shows a plot comparing the void fraction model to the data. In general, the agreement between the model and the data improved for qualities greater than 2×10^{-2}.

Adiabatic two-phase friction multiplier

To determine if the mass velocity had an effect on the two-phase friction multiplier the data were plotted in such a way as

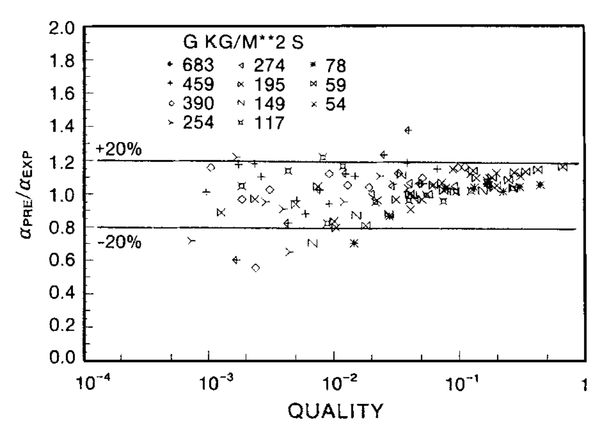

Figure 5. Predicted and experimental adiabatic void fraction data.

to (ideally) eliminate all effects except those associated with the mass velocity. The values of ϕ_ℓ^2 were plotted against the Martinelli parameter, Eq. 2, evaluated using the value of the Blasius exponent appropriate for each test run. The values of ϕ_ℓ^2 were also plotted, Figure 6, against the Martinelli parameter, calculated using a constant $m = 0.2$. Comparison of these two plotting schemes showed that when $m = 0.2$ the two-phase friction multiplier data exhibited far less scatter than when m was allowed to vary. The use of a constant value of m to evaluate a diverse data bank, where it is likely that a range of values of m would be more applicable, has been done by Ishihara et al. (1979). In that study the authors assumed that $m = 0.2$ would not be a bad approximation for most tube layouts over the range of $10^3 \leq Re \leq 10^5$. This approach was also adopted in the present study of the two-phase friction multiplier data both because of convenience and more well-behaved data curves.

As shown in Figure 6, there were strong mass velocity trends in the two-phase friction multiplier data. The values of ϕ_ℓ^2 increased with increasing mass velocity at a given value of χ_{tt} up to a value of $\chi_{tt} \simeq 0.9$, after which a crossover occured and the ϕ_ℓ^2 data then decreased with increasing mass velocity. Although the data of this present study have the same trends as predicted by Eq. 1, the use of $C = 8$ as suggested by Ishihara et al. did not result in a good representation of the data; the average absolute deviation between the predictions of the two-phase friction multiplier and the experimental data was 41% and the data were overpredicted by an average of 17%. Assuming that a Martinelli model could be used to correlate the present ϕ_ℓ^2 data, Eq. 1 was solved for the C factor. As shown in Figure 7, the mass velocity effects as well as the crossover point are now clearly visible. It is interesting to note that at the crossover point, the C factor is approximately equal to eight, the same value obtained by Ishihara et al. Although the mass velocity effects on the C factor are clearly visible, the reason for the different trends in the data (both increasing and decreasing values of ϕ_ℓ^2 with increasing mass velocity) at different flow conditions is not readily explainable. However, the two-phase friction multiplier has been observed (Chisholm, 1983; Wallis, 1972) to be a function of flow pattern. It is likely that the different data trends are the result of a change in flow pattern.

To observe the effects of flow pattern on the two-phase friction multiplier, the C factors were separated according to what flow pattern was present. While visibility of the tube bundle was

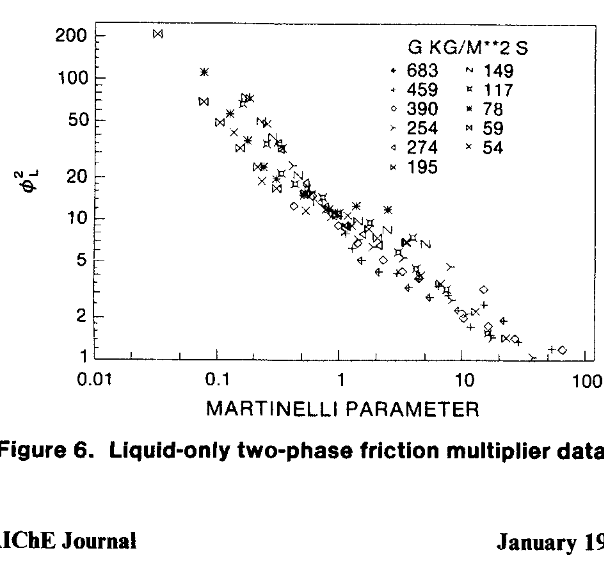

Figure 6. Liquid-only two-phase friction multiplier data.

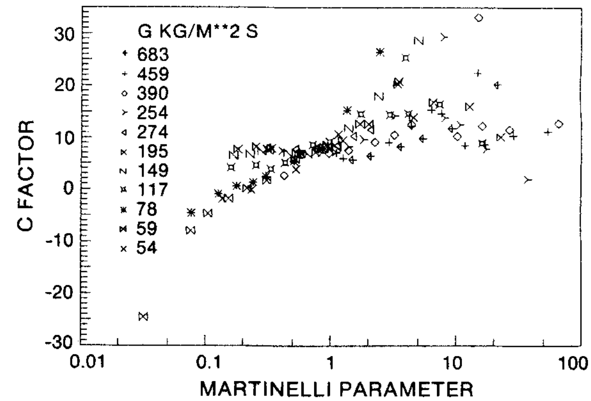

Figure 7. *C* factors reduced using Martinelli-type model.

somewhat limited because of the hardware used in the void measurement, the flowing mixtures generally could be classified as either bubbly, slug, or spray flow. Because of the difficulties associated with quantifying the flow patterns, the flow pattern map developed by Grant and Chisholm (1979) was used to classify the flows. Because of uncertainties in flow pattern transitions, any data point that was within 15% of a transition curve was, for data manipulation purposes only, assumed to be in both flow patterns. As a result, some data were plotted more than once, allowing data trends to be more easily established. Using this breakdown, the C factors plotted against χ_{tt} for each flow pattern can be found in Figure 8. The C factors plotted in this fashion clearly exhibit the dependence of mass velocity and flow pattern on the two-phase friction multiplier. For the data in both spray and slug flow patterns, ϕ_ℓ^2 increased with increasing mass velocity for a given value of χ_{tt}. However, in the bubbly flow pattern ϕ_ℓ^2 decreased with increasing mass velocity. The fact that this trend is evident in these bubbly flow data explains the crossover observed in Figures 6 and 7.

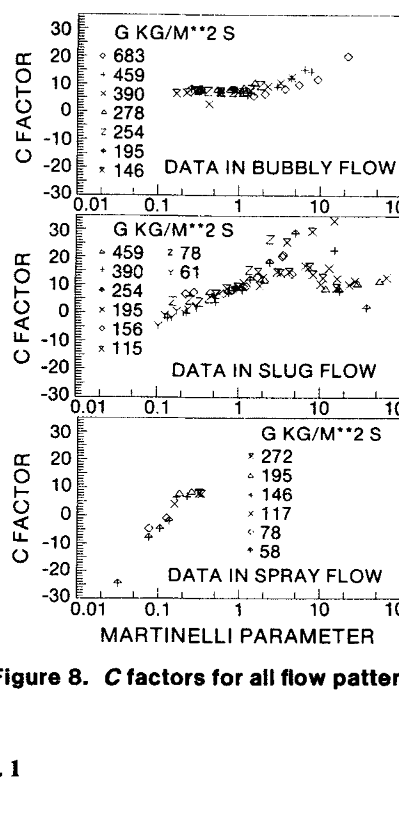

Figure 8. *C* factors for all flow patterns.

Suggestions for the reasons for these trends are as follows. In bubbly flows, an increase in mass velocity results in the generation of more turbulence, which acts to break up large bubbles into smaller pieces. The two-phase mixture behaves similar to a homogeneous fluid, with the vapor phase having less significance as quality decreases; hence, the frictional pressure characteristics approach those of a single-phase flow. By increasing the mass velocity the mixture behaves more like a homogeneous fluid, and the two-phase friction multiplier will subsequently decrease, as shown by the data. In a shell-side spray flow a liquid film covers each tube and travels over each row by spraying to the next tube downstream. In this process it is likely that a rough irregular interface exists between the gas and liquid phase, creating large interfacial drag forces that are further increased by a momentum exchange during entrainment and deposition of liquid drops between the liquid film on the tubes and the gas core. With increasing mass velocity, the liquid film on the tubes becomes even more wavy, contributing to higher frictional losses, and the rate at which the deposition and entrainment process occurs also increases. Thus, increases in the mass velocity will result in an increase in the two-phase friction multiplier, as observed in this study. The physical processes occurring in a shell-side slug flow are suggested to be an extension of those occurring in spray flow. Increasing the mass velocity would cause the large slugs to be broken up and the slug flow behavior would approach that of spray flow, which would account for the two-phase friction multiplier increasing with mass velocity.

To correlate the two-phase friction multiplier data, the C factor for each flow pattern was expressed as a function of χ_{tt} and G where:

$$C = (C_1 G^{C_2}) \ln \chi_{tt} + C_3 G^{C_4} \tag{6}$$

In the Ishihara et al. (1979) model the only coefficient subject to adjustment was that on the $1/\chi_{tt}$ term; this term had a coefficient of unity. The C factors in each flow pattern were initially correlated using Eq. 1 without a coefficient on the $1/\chi_{tt}^2$ term. This was the form of the C factor plotted in Figure 8. However, by introducing an additional coefficient, C_5, on the $1/\chi_{tt}^2$ term, a significant improvement could be made compared to the original form of the Ishihara et al. model, with the C factor given by Eq. 6. The final form of the correlation was:

$$\phi_\ell^2 = 1 + C/\chi_{tt} + C_5/\chi_{tt}^2 \tag{7}$$

Since Eq. 7 is a dimensional equation in mass velocity, the G terms were required to have units of $kg/m^2 \cdot s$. Table 1 shows the resulting curve fits, while Table 2 shows the comparison of each correlation with the experimental data. As can be seen, the agreement is good. A scatter band plot of the two-phase friction multiplier data is shown in Figure 9.

Table 1. Correlation Results for Dimensional Liquid-Only Two-Phase Friction Multiplier, Eqs. 6 and 7

Flow Pattern	C_1	C_2	C_3	C_4	C_5
Bubbly	7.34×10^{-6}	1.51	10.7	−0.057	0.774
Slug	81.4	−0.643	3.12	0.233	1.09
Spray	1,180	−1.50	3.87	0.207	0.205

Table 2. Comparison of Two-Phase Friction Multiplier Model with Experimental Data

Flow Pattern	N	$\frac{1}{N}\left(\sum_{i=1}^{N}\left\lvert\frac{\phi_{\ell pred}^2}{\phi_{\ell exp}^2} - 1\right\rvert\right)$	$\frac{1}{N}\left[\sum_{i=1}^{N}\left(\frac{\phi_{\ell pred}^2}{\phi_{\ell exp}^2}\right)\right]$
Bubbly	37	0.110	0.961
Slug	65	0.169	1.040
Spray	7	0.070	0.970
All patterns combined	109	0.143	0.999

It was found that the two-phase friction multiplier correlations for the slug and spray flow patterns would give values of ϕ_ℓ^2 that were less than unity if $G < \sim 43$ $kg/m^2 \cdot s$. No problem was found with the bubbly flow correlation. Hence, the present spray and slug flow correlations were restricted to flow conditions where $G \geq 43$ $kg/m^2 \cdot s$; for any mass velocity less than 43 $kg/m^2 \cdot s$ it was decided that the Ishihara et al. model should be applied.

The pressure drop associated with the inlet and exit geometries of the tube bundle was also addressed. This additional pressure drop is attributed to the sudden contraction and expansion of the two-phase mixture as it enters and leaves the tube bundle. As described by Schrage (1986), it was concluded that for all practical matters, inlet and exit losses could be considered negligible.

Simulated diabatic void fraction

The void fraction measured during the simulated diabatic two-phase flow tests represented the average void fraction for the quality and mass velocity ranges for any particular test. (Both quality and mass velocity increased between the inlet and exit of the bundle because of the air addition at each row). The void fraction correlation was integrated numerically over mass velocity and quality to give an average void fraction for the same range of conditions as in the experiment. Figure 10 shows a scatter band plot of the comparison between the average measured void fraction and the predicted values. For the outlet qualities greater than about 0.05 there was excellent agreement between the integrated void fraction model and the measured value. At higher mass velocities ($G \geq 678$ $kg/m^2 \cdot s$) and low qualities the integrated model overpredicted the data; however, at these con-

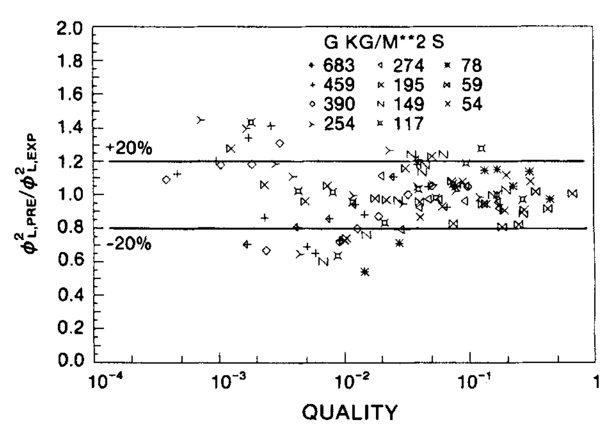

Figure 9. Predicted and experimental adiabatic liquid-only two-phase friction multiplier data.

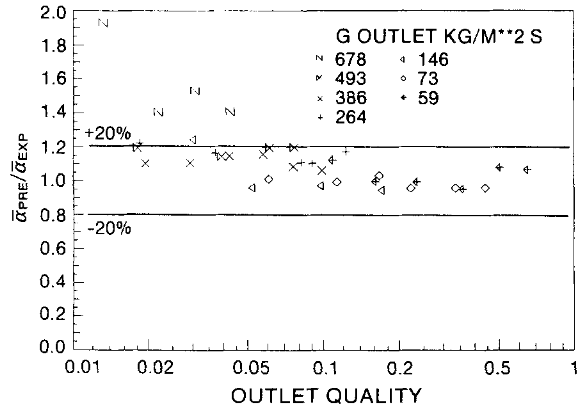

Figure 10. Predicted and experimental simulated diabatic void fraction data.

ditions the total pressure drop was dominated by the frictional and the liquid hydrostatic components. Hence, poor predication of the integrated void fraction model will not have a significant effect on the overall predicted pressure drop. Considering all of the data, the average absolute deviation between the predictions of the average void fraction and the experimental data was 15.3%. Neglecting the four data points for $G = 678$ kg/m^2 · s, the average absolute deviation between the predictions of the void fraction and the experimental data was 10.1%.

Simulated diabatic total pressure drop

Using both the integrated forms of the void fraction and the two-phase friction multiplier and the local flow conditions, the total pressure drop across the entire tube bundle could be predicted; this was then compared with the experimentally measured values. Figure 11 shows a comparison between the predicted and experimental total pressure drop. The average absolute deviation between the predictions and experimental data was 11.2%; the largest deviation encountered was only -22.8%. The average ratio of the predicted to experimental values was 1.00. The data that were taken with a high outlet quality condition were subjected to large increases in mass velocity between the inlet and exit of the tube bundle. Under these irregular flow conditions the data were still predicted with very good results. For one set of data, having an outlet quality of 0.65 with a factor

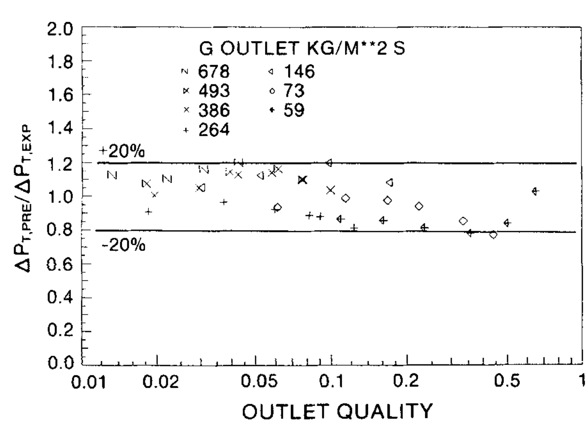

Figure 11. Predicted and experimental simulated diabatic total pressure drop data.

of three increases in local mass velocity between the inlet and outlet of the bundle, the total pressure drop was predicted within 2.8% of the measured value and the void fraction was predicted within 6.8%. The generally good prediction of this data would tend to add validity to the observed effects of mass velocity in the adiabatic two-phase friction multiplier and void fraction model.

R-113 diabatic total pressure drop

The diabatic total pressure drop data from an experiment using R-113 as the working fluid were also predicted with the present void fraction and two-phase friction multiplier models. The test section and experiment are described in detail by Jensen and Hsu (1987). Briefly, the test section had the same dimensions as the test section used in the present experiment; the channel was constructed from brass and all the tubes were stainless steel. The 135 tubes were electrically heated and were set at the same heat flux. The pressure drop across the complete bundle was measured with U-tube manometers. The ranges of experimental conditions for the 110 test runs were:

$1.6 \leq q'' \leq 44.1$ kW/m^2
$0 \leq x \leq 36\%$
$200 \leq P \leq 500$ kPa
$50 \leq G \leq 675$ kg/m^2 · s

By comparison of these data and the void fraction and two-phase friction multiplier models given above and with guidance from the literature, the mass velocity terms in both the void fraction model, Eq. 5, and two-phase friction multiplier model, Eq. 7, were nondimensionalized in terms of a Froude number. (Chisholm, 1983, and Whalley and Butterworth, 1983, both used a Froude number in describing the two-phase pressure drops in tube bundles.) Thus, revised coefficients for use in the nondimensionalized two-phase friction multiplier correlation, Eq. 8, are given in Table 3 and the nondimensional void fraction is given in Eq. 9.

$$C = (CFr_1^{C_2}) \ln \chi_{tt} + C_3 Fr^{C_4} \tag{8}$$

$$\alpha/\alpha_H = 1 + 0.123\, Fr^{-0.191} \ln x \tag{9}$$

An empirical single-phase friction factor obtained from single-phase flow data from this test selection was used along with the integrated void fraction and two-phase friction multiplier models from this study to predict the total pressure drop. A scatter plot of the predictions is given in Figure 12. The average abso-

Table 3. Coefficients in Nondimensional Two-Phase Friction Multiplier Correlation, Eqs. 7 and 8

Flow Pattern	C_1	C_2	C_3	C_4	C_5
Bubbly	0.036	1.51	7.79	−0.057	0.774
Slug*	2.18	−0.643	11.6	0.233	1.09
Spray*	0.253	−1.50	12.4	0.207	0.205

*If $Fr \leq 0.15$, use Ishihara et al. (1979) correlation
if $B \geq F_1$ Spray
if $B < F_1$ and $B < F_2$ Slug
if $B < F_1$ and $B \geq F_2$ Bubbly
where $F_1 = 0.678 A^{0.354}$
$F_2 = 1.86 A^{-1.93}$
$A = u_\ell^* (\rho_\ell \mu_\ell)^{1/3}/\sigma\, (1/\mathrm{N})^{1/3}$
$B = u_v^* (\rho_v/\rho_\ell)^{1/2}$ m/s

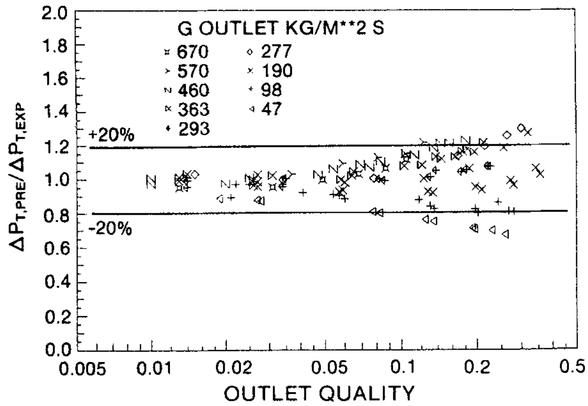

Figure 12. Predicted and experimental R-113 diabatic total pressure drop data.

lute deviation between the predictions and the experimental data was 9.8% and the average ratio of predicted to experimental total pressure drop was 0.99. Only one point was predicted with a deviation greater than 30%. This excellent agreement gives further support for the utility of the proposed correlations since the two fluids (R-113 and air/water) and experimental conditions are so significantly different. The one shortcoming of the proposed correlation is the apparent mass velocity shift. It is suspected that the flow pattern map used to identify the flow patterns is not general enough to accurately predict the flow patterns using R-113 and is contributing to the prediction trend shown in Figure 12. Work is continuing to improve the predictions.

Conclusions

In an experimental investigation void fractions and pressure drops were measured for two-phase vertical crossflow in a horizontal tube bundle. Both adiabatic and simulated diabatic, air-water, two-phase flows were tested over a large range of qualities and mass velocities. The adiabatic flow data were used to develop correlations for the void fraction and two-phase friction multiplier. Integrated over quality, these models were used to predict with good agreement the simulated diabatic void fraction and total pressure drop air-water data from this study and the R-113 diabatic total pressure drop data from a companion study.

The experimental data showed that the flow through the tube bundle was not a homogeneous flow and that the void fraction and two-phase friction multiplier are, respectively, functions of mass velocity and mass velocity and flow pattern. Because of the good agreement between the correlations and the predictions of the diabatic R-113 pressure drop data, it can be concluded that the quick-closing valve technique is an effective and valid method with which to measure void fractions in tube bundles.

Acknowledgment

This research is based on work supported by the National Science Foundation under Grant No. MEA-8319596.

Notation

A = abscissa in Grant and Chisholm flow pattern map, $(1/N)^{1/3}$
B = ordinate in Grant and Chisholm flow pattern map, m/s
C = C factor
C_1 to C_5 = correlation parameters, Eqs. 6, 8
D = tube diameter, m
f = single-phase friction factor, Eq. 3
F_1, F_2 = curves used to approximate Grant and Chisholm flow pattern map
Fr = $G/(\rho_\ell \sqrt{gD})$, Froude number
G = mass velocity based on minimum flow area, $kg/m^2 \cdot s$
g = gravitational constant, 9.806 m/s^2
M = number of tube rows between pressure taps
m = exponent in Blasius-type equation
ΔP = pressure drop, kPa
P = pressure, kPa
q'' = heat flux, W/m^2
u_ℓ^* = $G(1 - x)/\rho_\ell$, superficial liquid velocity, m/s
u_g^* = Gx/ρ_v, superficial vapor velocity, m/s
x = quality

Greek letters

α = void fraction
α_H = $1/\{1 + [(1 - x)/x)(\rho_v/\rho_\ell)]\}$ homogeneous void fraction
μ = dynamic viscosity, $kg/m \cdot s$
ρ = density, kg/m^3
σ = surface tension, N/m
ϕ^2 = two-phase friction multiplier
χ_{tt} = Martinelli parameter, Eq. 2

Subscripts

F = friction
ℓ = liquid phase only
ℓt = total flow assumed liquid
v = vapor phase only
1ϕ = single-phase
2ϕ = two-phase

Literature Cited

Chisholm, D., *Two-Phase Flow in Pipelines and Heat Exchangers*, Godwin, London (1983).
Diehl, J. E., "Calculate Condenser Pressure Drop," *Petrol. Refiner*, **36**(10), 147 (1957).
Diehl, J. E., and C. H. Unruh, "Two-Phase Pressure Drop for Horizontal Crossflow Through Tube Banks," ASME Paper No. 58-HT-20 (1958).
ESDU, "Crossflow Pressure Loss over Banks of Plain Tubes in Square and Triangular Arrays Including Effects of Flow Direction," Item No. 79034, Eng. Sci. Data Unit, London (1979).
Fair, J. R., and A. Klip, "Thermal Design of Horizontal Reboilers," *Chem. Eng. Prog.*, **79**(8), 86 (1983).
Frass, A. P., and M. N. Ozisik, *Heat Exchanger Design*, Wiley, New York (1965).
Grant, I. D. R., and D. Chisholm. "Two-Phase Flow on the Shell Side of a Segmentally Baffled Shell-and-Tube Heat Exchanger," *J. Heat Trans.*, **101**, 38 (1979).
Grant, I. D. R., I. C. Finlay, and D. Harris, "Flow and Pressure Drop During Vertically Upward Two-Phase Flow Past a Tube Bundle with and without Bypass Leakage," *I. Chem. E./I. Mech. E., Joint Symp. Multiphase Flow Systems, Univ. of Strathclyde, Glasgow, 2–4 April 1974*, Paper no. 17, Inst. Chem. Eng., London, 2 (1974).
Holman, J. P., *Experimental Methods for Engineers*, McGraw-Hill, New York (1984).
Ishihara, K., J. W. Palen, and J. Taborek, "Critical Review of Correlations for Predicting Two-Phase Pressure Drop Across Tube Banks," *Heat Trans. Eng.*, **1**(3) 1 (1979).
Jensen, M. K., and J.-T. Hsu, "A Parametric Study of Boiling Heat Transfer in a Tube Bundle," *Proc. 2nd ASME-JSME Thermal Eng. Joint Conf.*, P. J. Marto, I. Tanasawa, eds., ASME, **3**, 133 (1987).
Kays, W. M., and A. L. London, *Compact Heat Exchangers*, McGraw-Hill, New York (1984).
Kondo, M., and K.-I. Nakajima, "Experimental Investigation of Air-Water Two-Phase Upflow Across Horizontal Tube Bundles," *Bull. JSME*, **23**(177), 385 (1980).
Leong, L. S., and K. Cornwell, "Heat Transfer Coefficients in a Reboiler Tube Bundle," *Chem. Eng.*, No. 343, 219 (Apr., 1979).

Palen, J. W., and C. C. Yang, "Circulation Boiling Model for Analysis of Kettle and Internal Reboiler Performance," *Heat Exchangers for Two-Phase Applications,* HTD-Vol. 27, ASME, New York, 55 (1983).

Payvar, P., "Analysis of Performance of Full Bundle Submerged Boilers," *Two-Phase Heat Exchanger Symposium,* HTD-Vol. 44, ASME, New York, 11, (1983).

Polley, G. T., T. Ralston, and I. D. R. Grant, "Forced Crossflow Boiling in an Ideal In-line Tube Bundle," ASME Paper No. 80-HT-46 (1981).

Schrage, D. S., "Void Fraction and Two-Phase Pressure Drop in Crossflow in a Horizontal Tube Bundle," M.S. Thesis, Univ. Wisconsin, Milwaukee (Dec., 1986).

Wallis, G. B., *One-Dimensional Two-Phase Flow,* McGraw-Hill, New York (1972).

Whalley, P. B., and D. Butterworth, "A Simple Method for Calculating the Recirculation Flow in Vertical Thermosyphon and Kettle Reboilers," *Heat Exchangers for Two-Phase Applications,* HTD-Vol. 27, ASME, New York, 47, (1983).

Zhukauskas, A., "Heat Transfer from Tubes in Crossflow," *Adv. Heat Trans.,* **8,** 93 (1972).

Manuscript received Mar. 31, 1987 and revision received Aug. 24, 1987.